E ff ect of Sediment Gas Voids and Ebullition on Benthic Solute Exchange

DATASET · AUGUST 2015

READS
38

4 AUTHORS, INCLUDING:

Ronnie N. Glud
University of Southern Denmark
188 PUBLICATIONS **6,941** CITATIONS
SEE PROFILE

Katrin Premke
Leibniz-Institute of Freshwater Ecology and I…
25 PUBLICATIONS **333** CITATIONS
SEE PROFILE

Daniel Frank McGinnis
University of Geneva
79 PUBLICATIONS **1,662** CITATIONS
SEE PROFILE

Environmental Science & Technology

Article

pubs.acs.org/est

Effect of Sediment Gas Voids and Ebullition on Benthic Solute Exchange

Sabine Flury,[*,†,‡] Ronnie N. Glud,[‡,§,∥] Katrin Premke,[†,⊥] and Daniel F. McGinnis[†,‡,#]

[†]Chemical Analytics and Biogeochemistry, Leibniz-Institute of Freshwater Ecology and Inland Fisheries, 12587 Berlin, Germany

[‡]Nordic Centre for Earth Evolution (NordCEE), University of Southern Denmark, 5230 Odense M, Denmark

[§]Scottish Association for Marine Sciences, Scottish Marine Institute, PA37 1QA Oban, United Kingdom

[∥]Arctic Research Centre, University of Århus, 8000 Århus C, Denmark

[⊥]Institute for Landscape Biogeochemistry, Leibniz Centre for Agricultural Landscape Research (ZALF), 15374 Müncheberg, Germany

[#]Institute F.-A. Forel, Section of Earth and Environmental Sciences, Faculty of Sciences, University of Geneva, 1211 Geneva 4, Switzerland

Supporting Information

ABSTRACT: The presence of free gas in sediments and ebullition events can enhance the pore water transport and solute exchange across the sediment−water interface. However, we experimentally and theoretically document that the presence of free gas in sediments can counteract this enhancement effect. The apparent diffusivities (D_a) of Rhodamine WT and bromide in sediments containing 8−18% gas ($D_{a,YE}$) were suppressed by 7−39% compared to the control (no gas) sediments ($D_{a,C}$). The measured ratios of $D_{a,YE}$:$D_{a,C}$ were well within the range of ratios predicted by a theoretical soil model for gas-bearing soils. Whereas gas voids in sediments reduce the D_a for soluble species, they represent a shortcut for low-soluble species such as methane and oxygen. Therefore, the presence of even minor amounts of gas can increase the fluxes of low-soluble species (i.e., gases) by several factors, while simultaneously suppressing fluxes of dissolved species.

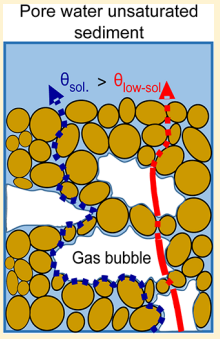

INTRODUCTION

Release of methane gas as bubbles (ebullition) is a natural phenomenon in aquatic systems, especially in shallow areas. [e.g., 1−3] Therefore, there is considerable interest in understanding how bubble formation, gas density, and gas release affect the interstitial transport of pore water constituents[4,5] such as nutrients,[5] pollutants,[6] and the net solute exchange across the sediment−water interface.[3,7]

Methane is formed as the last step of carbon mineralization in anoxic sediments and tends to accumulate in the pore water in the absence of oxidizing reagents.[8] Free gas bubbles will form in the pore water as the total dissolved gas partial pressure exceeds the local hydrostatic pressure. It is believed that bubbles form as eccentric oblate spheroids that fracture the sediment and subsequently rise along the formed cracks, eventually migrating upward and leaving the sediment.[9,10] At a given methane production, the ebullition events are often triggered by atmospheric and hydrostatic pressure drops,[11] changes in benthic shear stress,[12] and rising temperatures.[13]

Enhanced pore water fluxes at the sediment interface as measured by benthic flux chambers has often been attributed to bubble release.[6,14−16] Thus, several studies have investigated the effect of bubble migration and release on pore water exchange processes at the sediment−water interface. Klein[7] demonstrated up to 50% increased tracer flux in low-permeability sediments when introducing artificial bubble events, while O'Hara et al.[5] were able to show a nearly linear relationship between gas release rates and pore water advection in permeable sediments. According to Cheng et al.,[3] the extent to which pore water exchange is stimulated by ebullition in permeable sediment strongly depends on bubble size and the depth of bubble formation. However, these studies poorly reflect the situation in cohesive sediments.

In the absence of migrating bubbles, advection, or faunal activity, benthic solute transport is mainly driven by molecular diffusion.[17] The effective diffusivity of solutes in a porous media such as sediments depends on several factors: sediment type (cohesive or permeable), grain size, advection processes, presence of free gas, and compaction of the sediment,[17−19] and net transport of solutes is significantly reduced with increasing tortuosity (θ) (Figure 1). [e.g., 19−21]

Although it is well-recognized in soil science that the diffusivities of dissolved gases and solutes in porous media are strongly dependent on both the gas and water content, [e.g., 19,22] to our knowledge this is not addressed in sediment studies.

Received: April 20, 2015
Revised: July 23, 2015
Accepted: July 27, 2015

DOI: 10.1021/acs.est.5b01967
Environ. Sci. Technol. XXXX, XXX, XXX−XXX

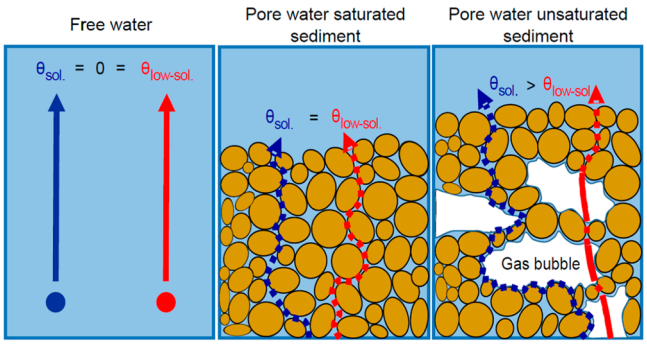

Figure 1. Tortuosity θ of a soluble (blue) and a low-soluble (red) pore water constituent (e.g., methane or oxygen), in free water (left panel), pore water saturated sediment (middle panel), and gas bearing, thus pore water unsaturated, sediment (right panel). The solid lines symbolize free diffusion in water (left panel) and gas (right panel), while dotted lines represent reduced diffusion by an increased tortuosity.

Characterization of transport processes in aquatic sediments charged with free gas [e.g., 3,23] often do not account for the potential impact of gas on solute transport.

In this study, we experimentally demonstrate how the presence of free gas significantly reduces the apparent diffusion of soluble species (e.g., bromide and Rhodamine WT), masking any potential bubble-mobilized pore water transport. Furthermore, using a theoretical model we demonstrate a significant simultaneous enhancement of diffusion of sparingly soluble substances (e.g., dissolved methane and oxygen) by the presence of free gases. The potential importance of these findings for the net exchange of solutes and gases in benthic settings is discussed.

MATERIALS AND METHODS

A total of four experiments were performed (Supporting Information Table SI 1): Two laboratory experiments (RWT experiment and Br experiment) were performed (i) to study the effect of gas presence on pore water exchange processes using tracer spiked sediment, (ii) to observe sediment expansion induced by the presence of gas, and (iii) to quantify the gas content. Two additional experiments (exp 1 and exp 2) were performed to solely (i) observe sediment expansion and (ii) quantify gas content. Each experiment included control tanks (i.e., with nonbubbling sediment) and actively bubbling tanks (i.e., with sediment methane production). In all instances, the initial sediment porosity was determined from the weight loss of a defined volume after drying at 60 °C until constant weight. The tanks were incubated in the dark at 20 (RWT experiment) and 27 °C (Br experiment).

Sediment Collection. *RWT Experiment.* Sediment was collected from the Odense River (Odense, Denmark). The 254-km^2 catchment mainly consists of agricultural soil.[24] Sediment was collected with a self-made push corer in February 2012 next to the outlet (55.37190 N, 10.38116 E) of a small, artificial, highly eutrophic pond located in Odense. Water depth at the sampling location was ~30−50 cm and the retrieved cores were ~30 cm long.

Br Experiment. Sediment was collected in December 2013 and in April 2014 from Lake Müggel (Berlin, Germany). Lake Müggel is a shallow, eutrophic lake with an average water depth of 4.9 m and a surface area of 750 ha.[25] The coring was performed with a UWITEC corer (diameter 10 cm) at a water depth of ~4 m, ~300 m offshore from the northern shoreline (52.44620 N; 13.65000 E). Retrieved sediment cores had a length of ~30−40 cm. Because the sediment surface was heavily colonized by clams and potential bioturbating fauna the top 5−10 cm was discarded.

Sediment Processing. *RWT Experiment.* Upon arrival at the laboratory, the sediment was sieved (mesh size ~2 × 2 mm) to remove fauna and rocks, etc. To inactivate remaining fauna, the sediment was frozen for a week at −20 °C. Methane production was stimulated by mixing 0.6% yeast extract (final pore water concentration; w/v) into the sediment for the "gas" producing tank (called YE tank from this point onward). Rhodamine WT (Keystone Europe Limited) was mixed into both the nonbubbling control (C) and the bubbling (YE) sediments as a tracer (final pore water concentration before sediment adsorption: ~500 μM). Rhodamine WT is considered biologically inert and nontoxic for microbes. [e.g., 26] Rhodamine WT adsorption tests were made to receive an estimate on potential binding of Rhodamine WT to the investigated sediments (for more details see SI 2 and Figure SI 1). As both tanks (control and actively bubbling tank) contained the same amount of sediment and tracer, the adsorption effect was the same and can be neglected for the calculations of apparent diffusivities.

Br Experiment. Lake Müggel sediment was sieved (mesh size 2 × 2 mm) to remove fauna. Half of the sediment was autoclaved and used for the control experiments. The other half was spiked with 0.8% (final pore water concentration; w/v) yeast extract to boost the natural methane production. Potassium bromide was added to both sediments as a tracer (10 mM final pore water concentration). Br^- is considered inert and often used for tracer studies in aquatic sediments. [e.g., 27]

Experimental Setup. *RWT Experiment.* Two incubation chambers (Table SI 1) were used: one control (C) and one actively producing and releasing bubbles (YE). The gastight tanks consisted of a square (26 × 26 × 49 cm) main body with a funnel-shaped lid that served as the gas trap (Figure SI 2). Two ports on the tank were connected to an external water bucket containing an EHEIM aquarium pump (5 L min^{-1} flow) to circulate the water. Rhodamine WT-amended sediment was placed in the chambers to a height of 13.5 cm. Thereafter, the chambers were completely filled and flushed ~3 times with tap water.

Br Experiment. This experiment was conducted with the two chambers described above, and an additional two circular chambers (Table SI 1). The circular chambers consisted of a main body (radius 9.2 cm, height 49 cm) and a funnel-shaped lid for gas entrapment (Figure SI 2). The sediment was filled in the chambers to a height of 15 cm and allowed to settle for 5 weeks (at 4 °C). The chambers were then carefully filled and flushed ~3 times with tap water.

Sediment Expansion Due to Gas. The measured sediment expansion was used to estimate the gas contents of the sediment for later modeling of the gas effect on diffusivities. To this end, the experimental setup was the same as for the Br experiment, with the exception of a 1−2-cm-high sand layer on top of the cohesive sediment to simulate different sediment layering. To account for the different sediment types and porosity effects, the sand layer was not considered part of the bulk sediment, but was considered separately when estimating the final gas and water contents of each sediment type.

DOI: 10.1021/acs.est.5b01967
Environ. Sci. Technol. XXXX, XXX, XXX−XXX

Chemical Analysis of Water Samples. Br^- was analyzed on diluted samples using an ion chromatograph (Dionex ICS 2000, Thermo-Fischer) according to DIN EN ISO 10204-1 (SI 4). The Rhodamine samples were taken 2−3 times a day and concentrations were determined spectrophotometrically at 500 nm after centrifugation of the water sample (SI 4).

Determination of Bubble Rate. Bubble rates (change of gas volume over time in funnel) were determined by either manually measuring the gas height in the cylindrical gas trap or by observing the changes on images taken by an infrared camera equipped with an LED infrared dark light source (SI 5).

Calculation and Definitions of Diffusivities. *Calculation of Apparent Tracer Diffusivity: D_a.* D_a is the apparent diffusivity that is derived from tracer fluxes (Table 1) and includes all combined processes: tortuosity related to both sediment particles and gas voids within the sediment, and any ebullition-enhanced pore water motion.

Table 1. Names and Meaning of Diffusivity (D) Terms Used in This Manuscript

D	meaning
D_w	diffusion coefficient in free water
$D_{s,s}$	diffusion coefficient in sediment saturated with pore water, corrected for sediment particles; for soluble species
$D_{s,ls}$	diffusion coefficient in sediment saturated with pore water, corrected for sediment particles; for low-soluble species
$D_{us,s}$	diffusion coefficient in gas bearing, and thus pore water unsaturated sediment, corrected for sediment particles and gas voids; for soluble species
$D_{us,ls}$	diffusion coefficient in gas bearing, and thus pore water unsaturated sediment, corrected for sediment particles and gas voids; for low-soluble species
D_a	apparent diffusion coefficient for the tracers; it includes the effect of sediment particles, gas voids, and pore water mixing by gas ebullition

To calculate the apparent diffusivity D_a, the baseline tracer flux ($J_{T,baseline}$; mg m^{-2} s^{-1}) before the onset of bubbling was determined from the accumulation rate of tracer mass in the overlying water over time (S_{bb}; mg s^{-1}) and per unit area (A; m^2) as

$$J_{T,baseline} = \frac{S_{bb}}{A} \quad (1)$$

Next, the baseline mass gradient $\Delta m_{baseline}$ across a square meter (mg m^{-3} m^{-1}) between the overlaying water and the sediment was determined as

$$\Delta m_{baseline} = \frac{J_{T,baseline}}{D_w} \quad (2)$$

with D_w (m^2 s^{-1}) as the known diffusivity of the tracer in free water adjusted to in situ temperature. D_{w,Br^-} was estimated to be 1.96×10^{-9} m^2 s^{-1} [8] and $D_{w,RWT}$ was approximated from D_w of Raffinose in water (3.20×10^{-10} m^2 s^{-1}).[26] Assuming that the concentration gradient after the onset of bubbling (at 193 h for RWT experiment, at 62 h for Br experiment; Figure 2) is equal to the gradient right before the bubbling. D_a (m^2 s^{-1}) can be calculated as

$$D_a = \frac{J_T}{\Delta m_{baseline}} \quad (3)$$

and

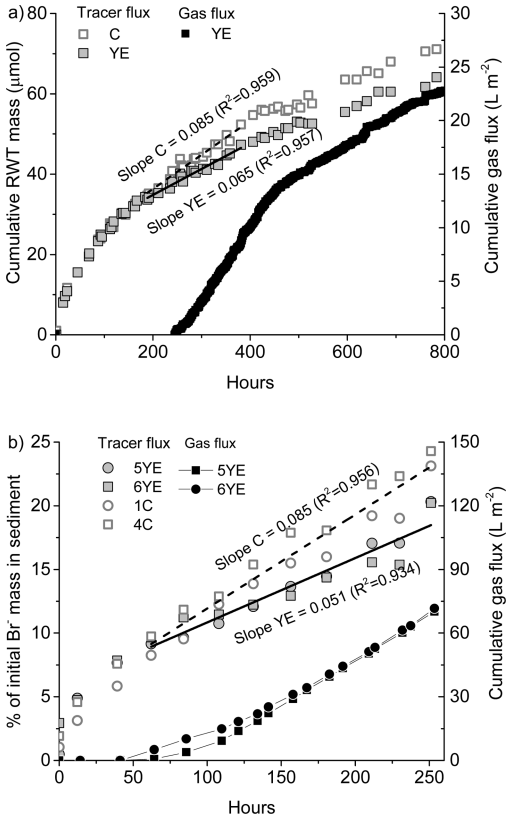

Figure 2. Tracer fluxes and gas fluxes of experiment (a) with Rhodamine WT and (b) with Br^- tracer. Linear curve fits include the period from the onset of constant gas production. Dashed line is the fitted curve for the controls, and the solid line represents the fitted curve for the tanks with ebullition.

$$J_T = \frac{S_b}{A} \quad (4)$$

with J_T as the tracer flux (mg m^{-2} s^{-1}) right when bubbling began, and S_b as the accumulation rate of tracer mass over time (S_b; mg s^{-1}) when bubbling began.

Diffusivities of Dissolved Species in Porous Media. Diffusivity of Dissolved Species in Pore Water Unsaturated Porous Media (D_{us}). D_{us} is defined as the diffusivity in gas-bearing and thus pore water unsaturated sediment (Table 1) based on the assumption that the pore space and the sediment grains have a spherical shape.[28] It includes the effect of sediment particles and gas voids and is estimated as[17,28]

$$D_{us} = D_w \cdot \frac{\alpha^{7/3}}{\varphi^2} \quad (5)$$

with α representing the volumetric water content and φ being the total porosity.

Diffusivity of Dissolved Species in Pore Water Saturated Porous Media (D_s). D_s is the diffusivity in sediment completely saturated with water (i.e., no gas) (Table 1). Thus, this includes only the effect of the sediment particles. D_s is calculated with eq 5 but with water content (α) equaling total porosity (φ). D_{us} and D_s will be further distinguished for soluble species (e.g., dissolved nutrients) ($D_{us,s}$ and $D_{s,s}$) and low-soluble species ($D_{us,ls}$ and $D_{s,ls}$).

To estimate $D_{us,ls}$, α is replaced by the volumetric gas content and D_w is replaced with the diffusivity of gases in free air.

DOI: 10.1021/acs.est.5b01967
Environ. Sci. Technol. XXXX, XXX, XXX−XXX

Table 2. Sediment Expansion, Water and Gas Content, and Calculated Diffusivities in Unsaturated Porous Media

expt	tank	sediment type[a]	initial height (cm)	final height (cm)	expansion (cm)	initial water content (%)	final calculated water content (%)	final calculated gas content (%)	total final porosity[b]	$D_{s,s}$[c] ($m^2\ s^{-1}$)	$D_{us,s}$[c] ($m^2\ s^{-1}$)	reduction of $D_{s,s}$ by gas[d] (%)
Br exp	5YE	1	15	20	5	90	81	10	0.91	1.88×10^{-09}	1.45×10^{-09}	23
Br exp	6YE	1	14.5	19.5	5	89	73	18	0.91	1.88×10^{-09}	1.13×10^{-09}	40
exp 2	3YE	1	14	15	1	88	82	7	0.89	1.88×10^{-09}	1.57×10^{-09}	16
RWT exp	6YE	2	13.5	14.6	1.1	43	40	8	0.48	2.42×10^{-10}	1.66×10^{-10}	31
exp 1	3YE	3	2	3	1	42	28	33	0.61	1.32×10^{-09}	2.40×10^{-10}	82
exp 1	5YE	3	2	2.5	0.5	42	34	20	0.54	1.32×10^{-09}	4.81×10^{-10}	64
exp 1	6YE	3	2	2.5	0.5	42	34	20	0.54	1.32×10^{-09}	4.81×10^{-10}	64
exp 2	3YE	3	1	2	1	42	21	50	0.71	1.47×10^{-09}	1.02×10^{-09}	93
exp 2	5YE	3	1	1.5	0.5	42	28	33	0.61	1.47×10^{-09}	2.67×10^{-10}	82
exp 2	6YE	3	1	1.5	0.5	42	28	33	0.61	1.47×10^{-09}	2.67×10^{-10}	82

[a]Sediment types are indicated by numbers: 1 = muddy lake sediment, 2 = sandy mud from Odense River, 3 = sand on top of muddy lake sediment. [b]Total final porosity = final gas content + final water content. [c]D is calculated based on Flury and Gimmi[17] with $D = (\alpha^{7/3}/\varphi^2)*D_w$. D_w taken from Schulz and Zabel[8] for Br^-, and from Glud and Fenchel[26] for RWT. [d]$D_{us,s}$ compared with $D_{s,s}$.

Table 3. Apparent Diffusivities for the RWT Experiment and Br Experiment

expt	tank pair	tracer	D_w ($m^2\ s^{-1}$)	D_a ($m^2\ s^{-1}$) C	D_a ($m^2\ s^{-1}$) YE	$D_{a,YE}:D_{a,C}$[a]	reduction of D_a by gas (%)[b]
RWT exp	square	Rhodamine WT	3.20×10^{-10}	2.58×10^{-10}	1.94×10^{-10}	0.75	25
Br exp	square	bromide	1.96×10^{-09}	1.44×10^{-09}	8.82×10^{-10}	0.61	39
Br exp	round	bromide	1.96×10^{-09}	1.37×10^{-09}	1.28×10^{-09}	0.93	7
mean Br exp[c]		bromide	1.96×10^{-09}	$1.41 \times 10^{-09} \pm 4.95 \times 10^{-11}$	$1.08 \times 10^{-09} \pm 2.81 \times 10^{-10}$	0.77 ± 0.23	23 ± 23

[a]Corresponds to $D_{us}:D_s$ in Figure 3. [b]C and YE compared. [c]The mean ± SD are reported for the Br exp.

RESULTS

Gas Fluxes. The RWT incubations ran for ~800 h, and ebullition began at ~245 h (Figure 2a). Initially, the gas flux increased rapidly, but reached a more stable rate after 200 h, followed by a slight reduction from 450 h to the experiment end. A total of 22 L m^{-2} of gas was released during the experiment, with an average bubble rate during the highest flux period of 1.6 L $m^{-2}\ d^{-1}$, and 0.7 L $m^{-2}\ d^{-1}$ during the low bubbling period (hour 450–800). As expected, no bubbles were observed or emitted in the control sediment.

The Br experiment was run for only 250 h as the bubbling started a few hours after incubation began (Figure 2b). Bubble rates were very similar for both replicates and reached a peak value of 9.4 L $m^{-2}\ d^{-1}$ after ~100 h, almost 6 times higher than the RWT experiment. This resulted in a total gas emission of 70 L m^{-2} over the experiment duration. As for the RWT experiment, the control sediment did not produce any noticeable gas or ebullition.

Gas and Water Content in Sediments. Methane production and the associated bubble accumulation within the top 2–10 cm led to a vertical expansion of the sediment. By visual observation, the shape of the initially formed bubbles (~1 mm diameter) was rather spherical and changed to flatter, oblate spheroids as they grew larger. Eventually, the bubbles merged and formed tubes and nonspherical shapes.

Although total porosity (total volume pore space/total volume sediment) increased due to the sediment extension by gas bubbles, the water content decreased (Table 2). The gas content in the muddy sediment varied between 7 and 18%, while it ranged from 20 to 50% in the sandy sediment layer (Table 2). In experiments 1 and 2, most of the gas produced in the muddy layer migrated up to the sandy layer and accumulated there. This led to an increased expansion of the sand layer, while the muddy sediment part (except for tank 3YE in experiment 2) did not expand noticeably.

Tracer Mass Fluxes. In both experiments, the tracer mass flux during gas formation and bubbling was considerably reduced (Figure 2). In the RWT experiment a 24% reduction (comparison of slopes between C and YE in Figure 2a) in mass flux was experienced ~3 days before the actual ebullition began. In the Br experiment the reduction appeared ~60 h into the experiment, which coincided with ebullition. On average the reduction in mass flux was 31% as compared to the control flux.

Apparent Diffusivities (D_a). Apparent diffusivities (D_a) during the bubbling phase were significantly reduced compared to the period immediately preceding bubbling. In the RWT experiment D_a was 39% lower than D_w, while in the Br experiment D_a was reduced by an average of 45% (±14% SD) compared to D_w (Table 3). Compared to the control sediment, the D_a was reduced on average by 24% (±16% SD) whereas the reduction in the RWT experiment was 25% and in the Br experiment 39% and 7% for the square and round tank, respectively (mean 23% ± 23% SD; Table 3).

Expected Diffusivities of Soluble Pore Water Species in Gas-Bearing Sediments: $D_{us,s}$. The expected $D_{us,s}$ values for Rhodamine WT and Br^- were calculated for porous unsaturated media according to the different water (and gas) contents from the sediment expansion experiments using eq 5 (Table 2, Figure 3). For normalization of the calculated diffusivities ($D_{us,s}$) and in order to include only the gas effect (but not the sediment particle effect) on D, the ratio of $D_{us,s}$ to $D_{s,s}$ was considered. $D_{us,s}:D_{s,s}$ is positively correlated with water content and negatively correlated with gas content (Figure 3). Furthermore, the effect of gas in sandy sediment on $D_{us,s}$

DOI: 10.1021/acs.est.5b01967
Environ. Sci. Technol. XXXX, XXX, XXX–XXX

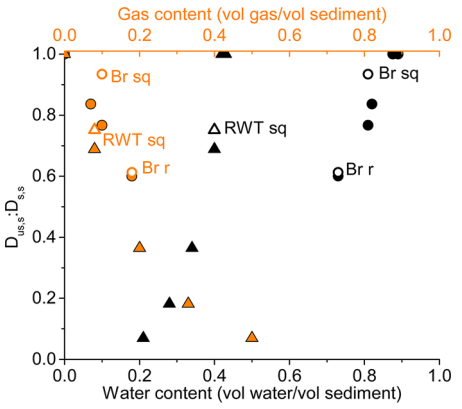

Figure 3. Effect of water and gas content on diffusivities of soluble species. To be able to compare the diffusivities of the different tracers, they are normalized to the diffusivities in water saturated sediment (D_s). Triangles correspond to data from sandy sediment, round symbols represent muddy sediment. Closed symbols present the expected $D_{us,s}$:$D_{s,s}$ ratios based on eq 5 and the estimated water and gas content from expansion experiments. Open symbols represent the ratios $D_{a,YE}$:$D_{a,C}$ from the tracer experiments (Table 3) in relation with the water and gas content of the corresponding experiments (Table 2).

follows an exponential function, while the effect in muddy sediment appears linear. The reduction of $D_{s,s}$ by gas (Table 2) is positively correlated with the gas content and was up to 90% when the gas was trapped in the sand layer.

DISCUSSION

Both investigated sediment types had an inherent natural gas production that led to ebullition (1.6–9.4 L m^{-2} d^{-1}), which is on the order of values encountered in natural systems.[3,13,29] However, in neither case did ebullition induce a net-enhancement of solute transport as would be expected from ebullition-driven pore water mixing. Contrarily, the presence of the bubbles resulted in a substantial suppression of the soluble tracer flux, even before ebullition occurred (RWT exp, Figure 2a) and during the ebullition phase (both experiments, Figure 2). This contrasts to previous laboratory experiments showing a 3–21 fold increase of tracer flux when bubbles were emitted from the sediment.[3,5,7] However, in these cases, the bubble events were induced artificially by inserting a needle into the sediment and injecting gas at a prescribed flow rate that was 4–70 fold[7] and 50–800 fold[3] higher than natural methane ebullition rates observed in aquatic systems.[3,13,29] Although investigations with such high bubble rates can represent an analog to ebullition from active seep sites, they poorly resemble conditions in natural freshwater sediments. We suggest that stationary bubbles in our experiments were responsible for the reduction in tracer fluxes by directly affecting the tortuosity for the dissolved substance. This aligns with previous work in water-logged peat soil, where a strong reduction of the hydraulic conductivity coincided with gas bubble accumulation.[30]

Effect of Free Gas Accumulation on D of Soluble Pore Water ($D_{us,s}$) Species and Tortuosity. The sediment expansion measurements allow us to calculate the change in total porosity, gas, and water content (Table 2).

Applying the soil equation, eq 5, and taking the free gas content from our experiments into account for determining $D_{us,s}$ (for, e.g., Br^- and RWT) clearly reveals that the free sediment gas (i.e., reduced water content) reduced the diffusivities of pore water-soluble species (Figure 3). Such an effect has been described in soil studies.[e.g., 19,31−33] In accordance with our findings (Figure 3), Lim et al.[33] also quantified a positive nonlinear relation of $D_{us,s}$ with water content in coarse-grained, and a positive linear relationship in fine-grained, porous media.

The pore water connectivity in porous media can be described as[19]

$$f_L = \frac{1}{\alpha} \cdot \frac{D_{us}}{D_w} \quad (6)$$

with f_L as the liquid-phase impedance factor, D_w as the diffusion coefficient of dissolved species in water, D_{us} as the diffusion coefficient of dissolved species affected by both sediment grains and gas voids (pore water unsaturated sediment), and α as the water content. Sediment type and grain size clearly affect the f_L, as finer grained sediments generally have a higher f_L than larger grained sediments. Thus, f_L in natural systems should be affected by different sediment layering. If f_L equals 0, the diffusion of soluble species is interrupted due to a disconnect of the liquid phase between the pores. Møldrup et al.[19] suggested a positive correlation between volumetric soil surface area and $\alpha_{threshold}$. In our study, this threshold value for the muddy sediment amounted to 0.3 (Figure 4a). This is slightly higher than the values (~0.06–0.2 for sand, loam, and clay) found by Møldrup et al.[19] presumably due to inclusion of much smaller grain sizes in the muddy sediment from Lake Müggel (Br

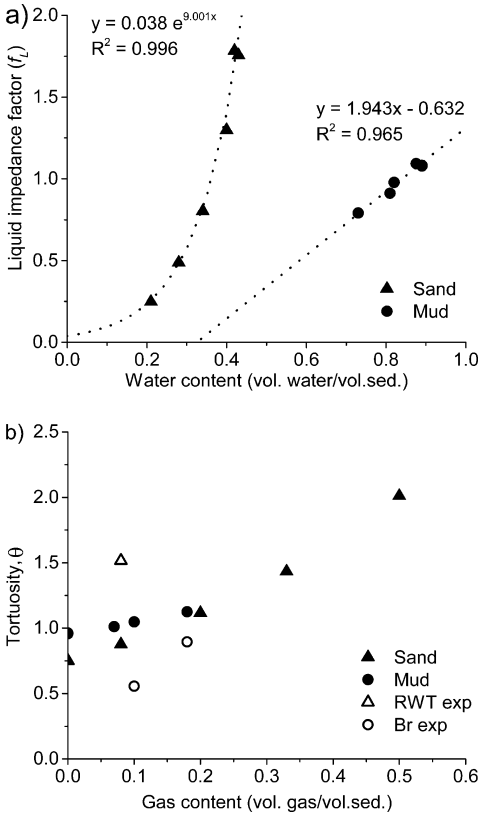

Figure 4. (a) Liquid-phase impedance factor (f_L) in relation to the water content eq 6. Dotted lines are fitted functions: exponential for sandy sediment and linear for fine-grained muddy sediment. (b) Tortuosity (= square root of $1/f_L$[19]) in relation with gas content. Open symbols are tortuosities calculated from the apparent diffusivities determined from the tracer experiments.

DOI: 10.1021/acs.est.5b01967
Environ. Sci. Technol. XXXX, XXX, XXX−XXX

experiment). However, the presence of ~60% free gas (corresponding to a water content of 0.3) in natural aquatic sediments is not likely. For sand and sandy mud it was not possible to determine such a threshold value since the function for f_L for sand (and sandy mud; i.e., RWT experiment) follows an exponential curve (Figure 4a). The estimated tortuosity (= square root of $1/f_L$[19]) is increasing with gas content (Figure 4b), thus confirming our hypothesis. These results are also in agreement with the soil results from Møldrup et al.[19]

The measured ratio $D_{a,YE}$:$D_{a,C}$ (Table 3, open symbols in Figure 3) fits well within the range of the expected ratios of $D_{us,s}$:$D_{s,s}$ calculated with the Millington–Quirk model (eq 5, Figure 3) despite the assumption of a rigid matrix for our sediments. For a more sophisticated approach, the elasticity of the sediment should be included in the model as, e.g., done in the soil model by Møldrup et al.[19] The fact that we were not able to observe an increased D_a following ebullition suggests that the naturally produced bubble rates in our systems were insufficient to enhance an observable net pore water exchange. However, that the tortuosities (open symbols in Figure 4b) estimated from apparent diffusivities do not perfectly fit with the theoretical tortuosities suggests other mechanisms at work (e.g., some bubble-driven pore water motion). Nevertheless, our results imply that the tortuosity effect of free-gas presence within the sediment impeded the net transport to the extent that it masked potential pore water release associated with ebullition. As the impedance factor f_L and $\alpha_{threshold}$ depend on sediment type and increases with volumetric soil surface (Figure 4 and[19]), this masking effect might be even stronger in impermeable fine-grained muddy sediments (this study) than in permeable sandy sediment.

Change in D for Sparingly Soluble Substances Due to Free Gas Accumulation within the Sediment: $D_{us,ls}$. Accumulation of gas voids at the sediment surface due to photosynthetically produced oxygen supersaturation[3,34,35] and in deeper layers due to methane supersaturation [e.g.,23] is a common phenomenon. As shown in Figure 1, gas voids within the sediment also affect the diffusivities of sparingly soluble gases such as oxygen, methane, other volatile organic carbons, and volatile trace metal species (e.g., Hg^0). While these gas voids impair diffusion for dissolved species, they significantly enhance sediment dissolved gas (low solubility) diffusivities. Instead of increasing the tortuosity (as for dissolved species), they provide short cuts for gases (Figure 1) entering the gas void. Considering that the diffusivity of a gas within air is on the order of 10^{-5} m^2 s^{-1} [17 and citations therein] gas voids locally increase the diffusivity by ~4 orders of magnitude (D for dissolved gas ~10^{-9} m^2 s^{-1}) (Figure 5). As an example, a gas content of only 7% increases $D_{us,ls}$ by more than 1 order of magnitude, while it increases by almost 2 orders of magnitude with 10% (Figure 5). Ignoring the existence of gas void when estimating diffusivities and gas fluxes therefore potentially leads to a large underestimation of $D_{us,ls}$ and thus of gas fluxes calculated from pore water concentration profiles.

Implications. Our results clearly demonstrate that accumulation of free gas affects the tortuosity of the sediment, and diffusion coefficients are subsequently overestimated for dissolved solutes and underestimated for sparingly soluble (i.e., dissolved gas) species. This has obvious consequences for the nutrient (and pollutant) exchange rate within the sediment, and at the sediment–water interface. In previous studies investigating sediment pollutant and nutrient exchange, fluxes measured by chambers often exceeded those calculated from pore water profiles.[6,14−16] The authors attributed these enhanced fluxes to methane bubbling. These fluxes can obviously be enhanced when bubbling rates are sufficiently high (e.g., at active seep sites[5]) or in permeable sediments with advective pore water transport. However, our results suggest that in natural (i.e., nonactive seep sites), cohesive methane-charged sediments, the enhancement of pore water exchange due to ebullition is likely masked by the strong impact of free stationary gas on the diffusivity of dissolved species. This leads to a substantial reduction of pore water exchange, especially in shallow areas where free gas can accumulate directly underneath the sediment surface. [e.g., 3,34,35] Therefore, in settings with intense eutrophication, gas formation and accumulation by stimulated benthic primary production (i.e., oxygen) and methane formation could actually reduce internal nutrient loading by hindering the release of nutrients from benthic mineralization. Nevertheless, the potential of the bubble-enhanced diffusion should be considered in relation to the magnitude of the bubbling rates and permeability of the sediment as the fluxes can indeed be enhanced with large bubble events in such settings.[5] Furthermore, also the EPS (extracellular polymeric substances) content could potentially indirectly affect diffusivity by influencing cohesiveness.

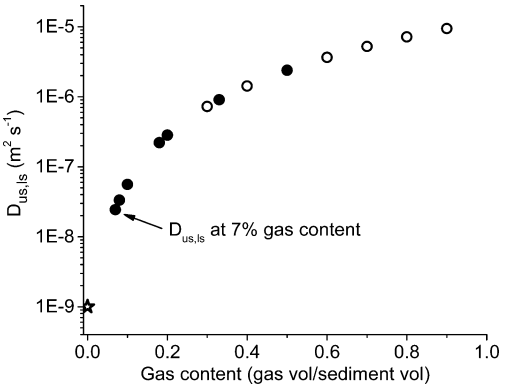

Figure 5. Effect of gas on D of any sparingly soluble species ($D_{us,ls}$) in gas-bearing sediments. The star symbol represents the approximate diffusivity of a gas dissolved in water and diffusing freely in water. Closed circles show $D_{us,ls}$ when applying eq 5 for the gas contents observed for the presented experiments (Table 2), where α is replaced by the gas content, and D_w by D in air. Open circles represent D for randomly assumed gas contents. Gas content is based on total sediment volume.

Gas voids in sediments will also strongly affect the hydraulics in sediments, especially in permeable sediment. Several investigations on gas bubbles in peat soils revealed a significant reduction of the hydraulic conductivity (2–8 times) when gas was present.[30,36] Strack et al.[37] suggest in their review paper that the reduced hydrological conductivity may affect the delivery of nutrients to biologically active sites. Similar effects can be expected for gaseous sediments, especially permeable (advective) sediments. Furthermore, sediment layering (i.e., changes from muddy to sandy sediment and vice versa) could potentially influence the overall hydraulics of the sediment as indicated by our observation that gas often accumulated at the interface of muddy and sandy sediment. For gas fluxes (e.g., oxygen, methane, dinitrogen, and hydrogen sulfide) this implies that even a small gas accumulation could significantly speed up gas fluxes in sediments, potentially increasing the carbon exchange rates.

DOI: 10.1021/acs.est.5b01967
Environ. Sci. Technol. XXXX, XXX, XXX−XXX

■ ASSOCIATED CONTENT

Supporting Information

The Supporting Information is available free of charge on the ACS Publications website at DOI: 10.1021/acs.est.5b01967.

Summary table of the experimental conditions (Table SI 1), the Rhodamine adsorption test (SI 2, Figure SI 1), a figure showing the setup of the experimental tanks (SI 3, Figure SI 2), a detailed description of bromide and Rhodamine WT analysis (SI 4), and a detailed description of the bubble rate determination (SI 5). (PDF)

■ AUTHOR INFORMATION

Corresponding Author

*E-mail: sabine.flury@yahoo.com; phone: +49 30 6418 1960; fax: +49 30 64181 700; Address: Leibniz-Institute of Freshwater Ecology and Inland Fisheries, Chemical Analytics and Biogeochemistry, Müggelseedamm 310, 12587 Berlin, Germany

Author Contributions

S.F. and D.F.M. conceived the study. S.F., D.F.M., R.N.G., and K.P. designed the experiments, and S.F. performed the experiment and data analysis with support from D.F.M.. S.F. wrote the manuscript. All 3 coauthors contributed to data discussion and writing.

Notes

The authors declare no competing financial interests.

■ ACKNOWLEDGMENTS

This work was supported by the Swiss National Science Foundation (Grant PA00P2_142041), the IGB-Fellowship Program, the German Research Foundation (DFG Grant LO 1150/5-1), the LandScales project (Leibniz association), The Commission for Scientific Research in Greenland (GCRC6507), European Research Council through an Advanced Grant (ERC-2010-AdG20100224), the Danish National Research Foundation (DNRF53 to Nordic Center for Earth Evolution), The Danish Council for Independent Research, and University of Southern Denmark. We also thank the mechanical workshop at the University of Southern Denmark for production of the sediment tanks, technicians from the Department of Chemical Analytics and Biogeochemistry at IGB-Berlin for measuring many Br^- and other samples, and Anni Glud and Morten Larsen for help with the initial experimental set up. Furthermore, we are grateful for the support by Jael Brüning and Amanda Cheng during the laboratory experiments.

■ REFERENCES

(1) Bastviken, D.; Cole, J.; Pace, M.; Tranvik, L. Methane emissions from lakes: Dependence of lake characteristics, two regional assessments, and a global estimate. *Global Biogeochem. Cycles* **2004**, *18* (4), No. GB4009.

(2) Flury, S.; McGinnis, D. F.; Gessner, M. O. Methane emissions from a freshwater marsh in response to experimentally simulated global warming and nitrogen enrichment. *J. Geophys. Res.* **2010**, *115* (G1), No. G01007.

(3) Cheng, C. H.; Huettel, M.; Wildman, R. A. Ebullition-enhanced solute transport in coarse-grained sediments. *Limnol. Oceanogr.* **2014**, *59* (5), 1733−1748.

(4) Haeckel, M.; Boudreau, B. P.; Wallmann, K. Bubble-induced porewater mixing: A 3-D model for deep porewater irrigation. *Geochim. Cosmochim. Acta* **2007**, *71*, 5135−5154.

(5) O'Hara, S. C. M.; Dando, P. R.; Schuster, U.; Bennis, A.; Boyle, J. D.; Chui, F. T. W.; Hatherell, T. V. J.; Niven, S. J.; Taylor, L. J. Gas seep induced interstitial water circulation - observation and environmental implications. *Cont. Shelf Res.* **1995**, *15* (8), 931−948.

(6) Canário, J.; Poissant, L.; O'Driscoll, N.; Vale, C.; Pilote, M.; Lean, D. Sediment processes and mercury transport in a frozen freshwater fluvial lake (Lake St. Louis, QC, Canada). *Environ. Pollut.* **2009**, *157* (4), 1294−1300.

(7) Klein, S. Sediment porewater exchange and solute release during ebullition. *Mar. Chem.* **2006**, *102* (1−2), 60−71.

(8) Schulz, H. D.; Zabel, M. *Marine Geochemistry*; Springer Verlag: Berlin, Heidelberg, New York, 2000; p 455.

(9) Algar, C. K.; Boudreau, B. P.; Barry, M. A. Initial rise of bubbles in cohesive sediments by a process of viscoelastic fracture. *J. Geophys. Res.* **2011**, *116* (B4), No. B04207.

(10) Boudreau, B. P.; Algar, C.; Johnson, B. D.; Croudace, I.; Reed, A.; Furukawa, Y.; Dorgan, K. M.; Jumars, P. A.; Grader, A. S.; Gardiner, B. S. Bubble growth and rise in soft sediments. *Geology* **2005**, *33* (6), 517−520.

(11) Comas, X.; Slater, L.; Reeve, A. S. Atmospheric pressure drives changes in the vertical distribution of biogenic free-phase gas in a northern peatland. *J. Geophys. Res.* **2011**, *116* (G4), No. G04014.

(12) Joyce, J.; Jewell, P. W. Physical controls on methane ebullition from reservoirs and lakes. *Environ. Eng. Geosci.* **2003**, *9* (2), 167−178.

(13) DelSontro, T.; McGinnis, D. F.; Sobek, S.; Ostrovsky, I.; Wehrli, B. Extreme methane emissions from a Swiss hydropower reservoir: contribution from bubbling sediments. *Environ. Sci. Technol.* **2010**, *44* (7), 2419−2425.

(14) Liikanen, A.; Huttunen, J. T.; Murtoniemi, T.; Tanskanen, H.; Vaisanen, T.; Silvola, J.; Alm, J.; Martikainen, P. J. Spatial and seasonal variation in greenhouse gas and nutrient dynamics and their interactions in the sediments of a boreal eutrophic lake. *Biogeochemistry* **2003**, *65* (1), 83−103.

(15) Klump, J. V.; Martens, C. S. Biogeochemical cycling in an organic rich coastal marine basin 2. Nutrient sediment water exchange processes. *Geochim. Cosmochim. Acta* **1981**, *45* (1), 101−122.

(16) Dale, A. W.; Bertics, V. J.; Treude, T.; Sommer, S.; Wallmann, K. Modeling benthic-pelagic nutrient exchange processes and porewater distributions in a seasonally hypoxic sediment: evidence for massive phosphate release by Beggiatoa? *Biogeosciences* **2013**, *10* (2), 629−651.

(17) Flury, M.; Gimmi, T. F. Solute diffusion. In *Methods of Soil Analysis, Part 4, Physical Methods*; Dane, J. H., Topp, G. C., Eds. Soil Science Society of America: Madison, WI, 2002; pp 1323−1351.

(18) Iversen, N.; Jørgensen, B. B. Diffusion-coefficients of sulfate and methane in marine sediments - Influence of porosity. *Geochim. Cosmochim. Acta* **1993**, *57* (3), 571−578.

(19) Moldrup, P.; Olesen, T.; Komatsu, T.; Schjonning, P.; Rolston, D. E. Tortuosity, diffusivity, and permeability in the soil liquid and gaseous phases. *Soil Sci. Soc. Am. J.* **2001**, *65* (3), 613−623.

(20) Saripalli, K. P.; Serne, R. J.; Meyer, P. D.; McGrail, B. P. Prediction of diffusion coefficients in porous media using tortuosity factors based on interfacial areas. *Groundwater* **2002**, *40* (4), 346−352.

(21) Carman, P. C. *Flow of Gas through Porous Media*; Academic Press: New York, 1956.

(22) Aachib, M.; Mbonimpa, M.; Aubertin, M. Measurement and prediction of the oxygen diffusion coefficient in unsaturated media, with applications to soil covers. *Water, Air, Soil Pollut.* **2004**, *156* (1−4), 163−193.

(23) Anderson, M. A.; Martinez, D. Methane gas in lake bottom sediments quantified using acoustic backscatter strength. *J. Soils Sediments* **2015**, *15*, 1246−1255.

(24) Poulsen, J. B.; Hansen, F.; Ovesen, N. B.; Larsen, S. E.; Kronvang, B. Linking floodplain hydraulics and sedimentation patterns along a restored river channel: River Odense, Denmark. *Ecol. Eng.* **2014**, *66*, 120−128.

(25) Hilt, S.; Koehler, J.; Adrian, R.; Monaghan, M. T.; Sayer, C. D. Clear, crashing, turbid and back - long-term changes in macrophyte

DOI: 10.1021/acs.est.5b01967
Environ. Sci. Technol. XXXX, XXX, XXX−XXX

assemblages in a shallow lake. *Freshwater Biol.* **2013**, *58* (10), 2027−2036.
(26) Glud, R. N.; Fenchel, T. The importance of ciliates for interstitial solute transport in benthic communities. *Mar. Ecol.: Prog. Ser.* **1999**, *186*, 87−93.
(27) Forster, S.; Glud, R. N.; Gundersen, J. K.; Huettel, M. In situ study of bromide tracer and oxygen flux in coastal sediments. *Estuarine, Coastal Shelf Sci.* **1999**, *49* (6), 813−827.
(28) Millington, R.; Quirk, J. P. Permeability of porous solids. *Trans. Faraday Soc.* **1961**, *57* (8), 1200−1207.
(29) Maeck, A.; DelSontro, T.; McGinnis, D. F.; Fischer, H.; Flury, S.; Schmidt, M.; Fietzek, P.; Lorke, A. Sediment trapping by dams creates methane emission hot spots. *Environ. Sci. Technol.* **2013**, *47* (15), 8130−8137.
(30) Beckwith, C. W.; Baird, A. J. Effect of biogenic gas bubbles on water flow through poorly decomposed blanket peat. *Water Resour. Res.* **2001**, *37* (3), 551−558.
(31) Olesen, T.; Moldrup, P.; Yamaguchi, T.; Rolston, D. E. Constant slope impedance factor model for predicting the solute diffusion coefficient in unsaturated soil. *Soil Sci.* **2001**, *166* (2), 89−96.
(32) Porter, L. K.; Kemper, W. D.; Jackson, R. D.; Stewart, B. A. Chloride diffusion in soils as influenced by moisture content. *Soil Sci. Soc. Am. J.* **1960**, *24* (6), 460−463.
(33) Lim, P. C.; Barbour, S. L.; Fredlund, D. G. The influence of degree of saturation on the coefficient of aqueous diffusion. *Can. Geotech. J.* **1998**, *35* (5), 811−827.
(34) Revsbech, N. P.; Jorgensen, B. B.; Brix, O. Primary production of microalgae in sediments measured by oxygen microprofile, H-CO-14(3)-fixation, and oxygen-exchange methods. *Limnol. Oceanogr.* **1981**, *26* (4), 717−730.
(35) Jørgensen, B. B.; Revsbech, N. P.; Cohen, Y. Photosynthesis and structure of benthic microbial mats - Microelectrode and SEM studies of 4 cyanobacterial communities. *Limnol. Oceanogr.* **1983**, *28* (6), 1075−1093.
(36) Baird, A. J.; Waldron, S. Shallow horizontal groundwater flow in peatlands is reduced by bacteriogenic gas production. *Geophys. Res. Lett.* **2003**, *30* (20), 2043.
(37) Strack, M.; Kellner, E.; Waddington, J. M. Dynamics of biogenic gas bubbles in peat and their effects on peatland biogeochemistry. *Global Biogeochem. Cycles* **2005**, *19* (1), GB1003.

DOI: 10.1021/acs.est.5b01967
Environ. Sci. Technol. XXXX, XXX, XXX−XXX